Progress in Natural Science: Materials International 2013;23(4):408–412

Chinese Materials Research Society

Progress in Natural Science: Materials International

www.elsevier.com/locate/pnsmi
www.sciencedirect.com

ORIGINAL RESEARCH

Effects of Ce, Y, and Sm doping on the thermoelectric properties of Bi_2Te_3 alloy

Fang Wu[a,b], Hongzhang Song[a], Jianfeng Jia[a], Xing Hu[a,*]

[a]*School of Physical Engineering, Zhengzhou University, Zhengzhou 450052, China*
[b]*Department of Physics, Henan Institute of Education, Zhengzhou 450053, China*

Received 8 December 2012; accepted 29 May 2013
Available online 18 July 2013

KEYWORDS

Elements doped;
$R_{0.2}Bi_{1.8}Te_3$;
Morphologies;
Figure of merit

Abstract Nanopowders of elements doped Bi_2Te_3 thermoelectric alloy $R_{0.2}Bi_{1.8}Te_3$ (R=Ce, Y and Sm) were synthesized by the hydrothermal method. The nanopowders were hot-pressed into pellets and their thermoelectric properties were investigated. The results show that Ce, Y, and Sm doping has significant effects on the morphologies of the synthesized nanopowders and thermoelectric properties. Among the doping elements, Ce doping is a superiority dopant. Although the electrical conductivity and Seebeck coefficient are not improved much by Ce doping, the thermal conductivity is supressed greatly. As a result the figure of merit (*ZT*) of $Ce_{0.2}Bi_{1.8}Te_3$ is improved and reaches 1.29 at 398 K, which is higher than the Bi_2Te_3 ingots made by the traditional zone-melting method

1. Introduction

Thermoelectric materials, which can generate electrical power from waste heat or be used as solid-state Peltier coolers, could play an important role in a global sustainable energy solution [1–3]. Fundamental research on the field of thermoelectric materials is to obtain materials with a high figure of merit (*ZT*). This in turn needs to optimize a variety of conflicting properties, such as Seebeck coefficient, electrical conductivity, and thermal conductivity. An ideal thermoelectric material should have a large Seebeck coefficient (absolute value), high electrical conductivity, and low thermal conductivity. As these transport characteristics are correlated with each other, obtaining a high *ZT* value is not an easy job [4,5]. In recent years, employing band engineering (usually through elements doping) and nanostructure engineering (reduce the size of the sample or grains in a bulk to nanoscale) to enhance the *ZT* value of thermoelectric materials have become a focus [6,7,8].

Bismuth telluride Bi_2Te_3 alloy is one of the best thermoelectric materials working at around room temperature. But the *ZT* values of the main commercial Bi_2Te_3 based alloys have remained around 1 for a long time [5]. During the past decades there were many

*Corresponding author.
E-mail address: xhu@zzu.edu.cn (X. Hu).

Peer review under responsibility of Chinese Materials Research Society.

ELSEVIER Production and hosting by Elsevier

http://dx.doi.org/10.1016/j.pnsc.2013.06.007

reports on the nanostructured bismuth telluride based alloys attempting to enhance their *ZT* values. Xie et al. [9] employed the melt spinning method combined with a subsequent spark plasma sintering technique to fabricate nanostructured p-type $(Bi,Sb)_2Te_3$ samples which showed a maximum *ZT* of 1.5 at about 390 K. Poudel et al. [10] found that a *ZT* value of 1.4 at 373 K could be achieved in a p-type nanocrystalline BiSbTe bulk alloy made by the ball-milling followed by hot-pressing. Cao et al. [11] utilized the hydrothermal method and hot-pressing to prepare nanostructured $(Bi,Sb)_2Te_3$ bulk samples which showed a high *ZT* value of 1.28 at 303 K. Compared with the progress of the p-type Bi_2Te_3-based alloys, the *ZT* value of n-type Bi_2Te_3 based alloys has not been improved much than 1 [12]. Because both p-type and n-type thermoelectric materials are essential for the fabrication of a thermoelectric device, it is also important to optimize the thermoelectric performances of n-type Bi_2Te_3-based alloys.

Based on the reports, the high *ZT* may be related to the inhomogeneities on various length scales of the bulk. And the thermoelectric properties of nanostructured materials should depend on the size and morphology of the microstructural features [5]. In our previous study (not shown here), we synthesized n-type Bi_2Te_3 nanosheets with flower-like shape by the hydrothermal method and found a *ZT* value of 1.16 can be achieved at 423 K which was resulting in from a suitable microstructure. As mentioned above, element doping is also an effective way to improve the figure of merit. To further improve the figure of merit, a combination of the band engineering and nanostructure engineering techniques should be effective. In the present paper we report the synthesis of elements doped n-type $R_{0.2}Bi_{1.8}Te_3$ (R = Ce, Y and Sm) nanopowders using the hydrothermal method and investigate the thermoelectric properties of the bulk samples made by these nanopowders. We found that the doping of these rare earth elements can decrease the thermal conductivity, especially for the Ce element doped sample. As a result the *ZT* value of the Ce doped sample can reach 1.29 at 373 K.

2. Experimental

The hydrothermal method was used to synthesize Bi_2Te_3 and $R_{0.2}Bi_{1.8}Te_3$ nano-powders. In a typical experiment running, 40 ml aqueous solution containing 1.8 mmol $BiCl_3$, 0.2 mmol $Ce(NO_3)_3 \cdot 6\,H_2O$ (or $Y(NO_3)_3 \cdot 6\,H_2O$ and $Sm(NO_3)_3 \cdot 6\,H_2O$), 3 mmol tellurium powders, 0.2 g ethylenediamine tetra acetic acid (EDTA) and some sodium hydroxide (NaOH) were mixed in an open beaker. The mixture was stirred with a magnetic stirrer for 0.5 h, then 0.35 g $NaBH_4$ was introduced into the solution. The mixed solution was moved into a Teflon-lined autoclave, and then sealed and maintained at 423 K for 24 h. The resulting powders were filtered off and washed several times using distilled water, absolute ethanol, and acetone. Then the powders were dried in a vacuum box at 373 K for 6 h. The resultant powders were hot-pressed into pellets with a diameter of 15 mm or 12.5 mm and thickness about 2 mm at 773 K for 15 min under a pressure of 60 MPa in vacuum.

The phases of the obtained $R_{0.2}Bi_{1.8}Te_3$ (R = Ce or Y and Sm) nanopowders were identified by X-ray diffraction (XRD) using an X'Pert Pro diffractometer (PANalytical, The Netherlands). The morphologies of the powders were observed by field-emission scanning electron microscopy (FESEM) on a JSM-6700F microscope (JEM; JEOL, Tokyo, Japan). The electrical conductivity and the Seebeck coefficient of rectangle bars cut from the ϕ15 mm pellets were measured at several temperature points by using a LSR-3/800 Seebeck coefficient/electric resistance measuring system (LINSEIS, Germany) under He atmosphere. The thermal conductivity of the ϕ12.5 mm pellets was measured by a thermal diffusivity system (FLASHLINETM 3000, ANTER Corporation, USA) using Pyroceram (Provided by ANTER) as a reference sample at several temperature points. The measured direction of the electrical conductivity and the Seebeck coefficient is perpendicular to the pressing direction (the direction of the radial direction of the ϕ15 mm pellets), while the measured direction of the thermal conductivity is parallel to the pressing direction (along the direction of the thickness of the ϕ12.5 mm pellets). This choice of the measured directions is limited by the size of the samples. But according to the reports of Poudel et al. [10] the thermoelectric properties should be isotropic if the orientations of the grains in hot-pressed bulk samples are random.

3. Results and discussion

Fig. 1 shows the XRD patterns of the obtained nanopowders. All the reflection peaks of the powders can be indexed to the rhombohedral Bi_2Te_3, and no remarkable impure phases such as tellurium, bismuth, cerium (or yttrium and samarium) or their other compounds are observed. It is believed that Ce (or Y and Sm) has entered the lattice of Bi_2Te_3. The lattice constants of the samples are calculated by Rietveld refinement and are shown in Table 1. It can be observed that the lattice parameters $R_{0.2}Bi_{1.8}Te_3$ are all slightly higher than Bi_2Te_3. The little change for the crystal constant can be attributed to the small differences between the atomic radii of cerium (1.85 Å), yttrium (1.80 Å), samarium (1.85 Å) and bismuth (1.60 Å).

Fig. 2 shows the morphologies of the synthesized nanopowders observed by SEM. It can be observed that when doping with rare earth elements, the morphologies of the nanopowders change greatly. As shown in Fig. 2(a) the sample without rare earth elements doping shows flower-like shape. As shown from Fig. 2 (b) to (d), when doping with Ce, Y and Sm, the nano-sheets become smaller. It indicates that rare earth elements doping have significant effect on the morphologies of the powders. It is not very clearly known at present why rare earth elements doping can change the morphologies significantly. The possible reason may be

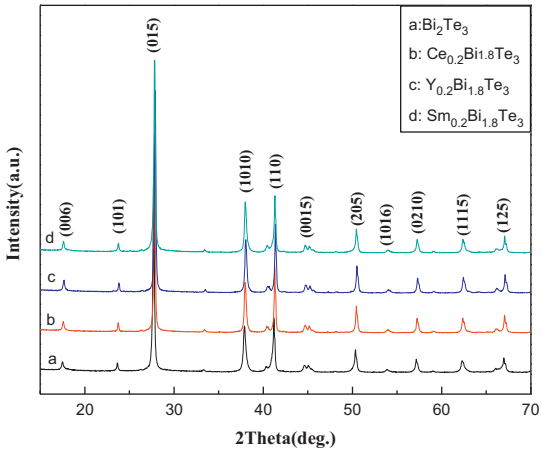

Fig. 1 XRD patterns of the synthesized powders (a) Bi_2Te_3; (b) $Ce_{0.2}Bi_{1.8}Te_3$; (c) $Y_{0.2}Bi_{1.8}Te_3$ and (d) $Sm_{0.2}Bi_{1.8}Te_3$.

Table 1 Lattice parameters of the synthesized powders.

Sample	Bi_2Te_3	$Ce_{0.2}Bi_{1.8}Te_3$	$Y_{0.2}Bi_{1.8}Te_3$	$Sm_{0.2}Bi_{1.8}Te_3$
a (Å)	4.382	4.387	4.382	4.386
c (Å)	30.485	30.495	30.492	30.496

that the replacement of Bi by rare earth elements can change the bonds strength and affect the growth rate along *a*-axis, *b*-axis and *c*-axis.

Fig. 3 shows the microstructures of the hot-pressed bulk samples. As shown in Fig. 3, there are no obvious orientations of the grains in the hot pressed bulks. It can be seen that the Bi_2Te_3 is more compact than others. It is evident that all samples have

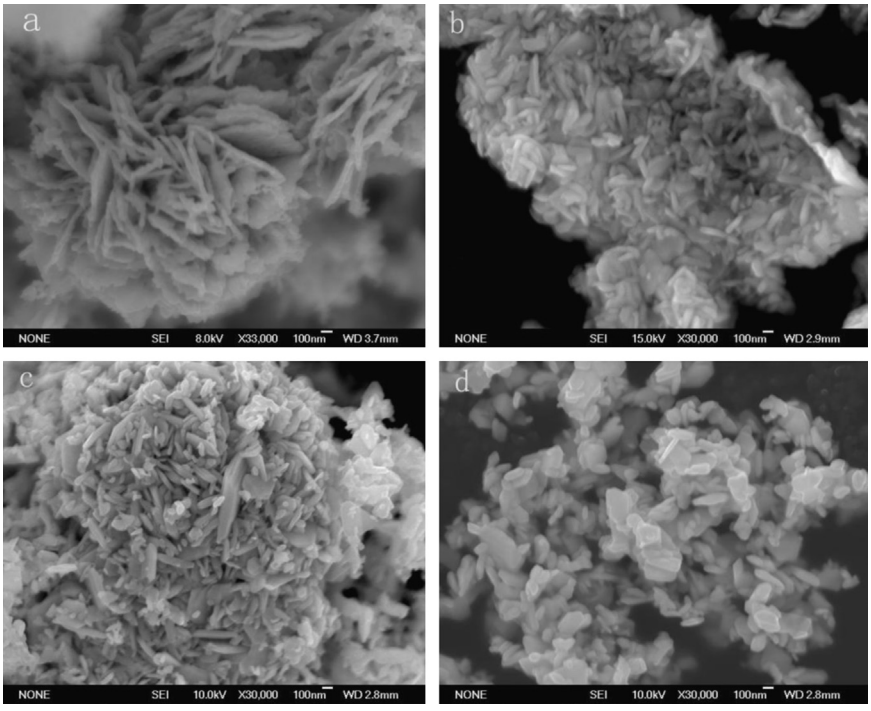

Fig. 2 SEM images of the nanopowders (a) Bi_2Te_3, (b) $Ce_{0.2}Bi_{1.8}Te_3$, (c) $Y_{0.2}Bi_{1.8}Te_3$ and (d) $Sm_{0.2}Bi_{1.8}Te_3$.

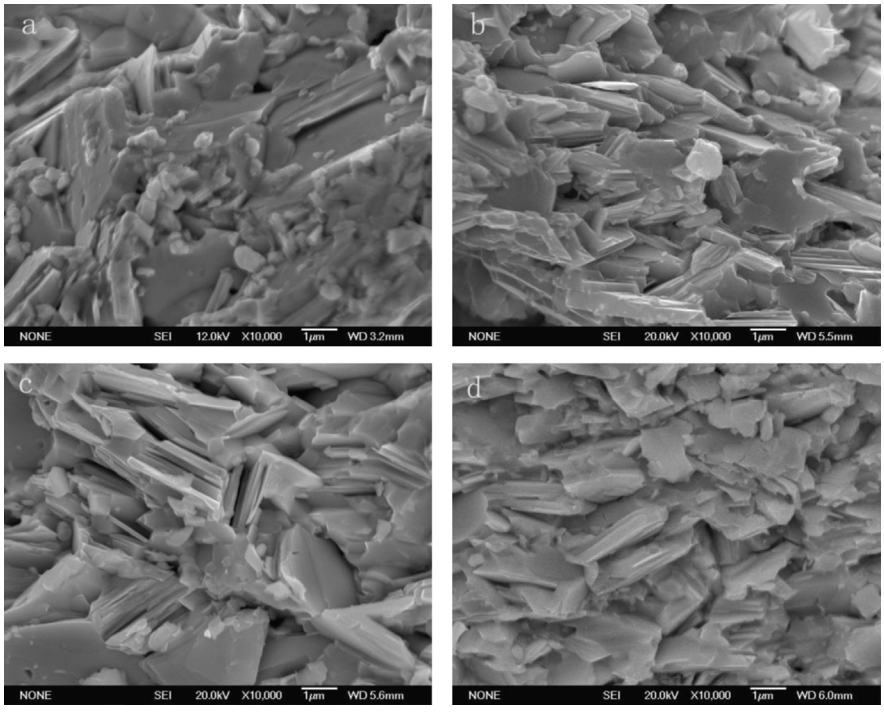

Fig. 3 SEM images of the hot-pressed samples (a) Bi_2Te_3, (b) $Ce_{0.2}Bi_{1.8}Te_3$, (c) $Y_{0.2}Bi_{1.8}Te_3$ and (d) $Sm_{0.2}Bi_{1.8}Te_3$.

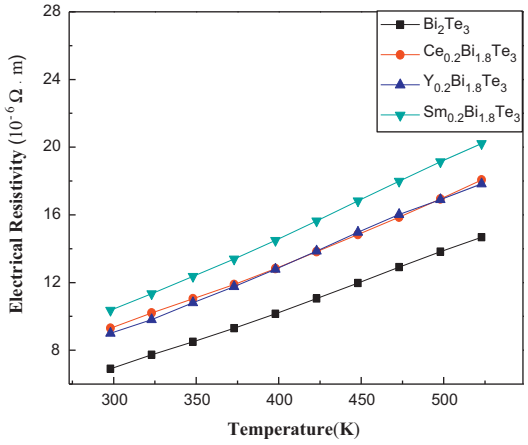

Fig. 4 Electrical resistivity of the hot-pressed samples.

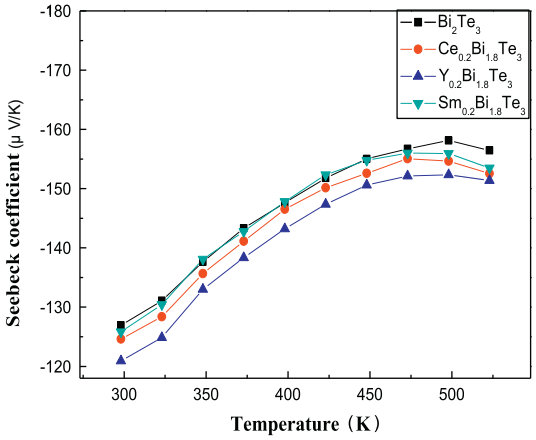

Fig. 5 Seebeck coefficients of the hot-pressed samples.

similar sheet-shaped microstructures. The sheet crystals significantly grew up during the hot pressing. However, the thickness of the sheet crystals is still lower than 100 nm, which should be beneficial to the improvement of the thermoelectric properties. Among the samples, the sheet crystals of the Bi_2Te_3 are much lager and thicker than others. For all samples, there are some tiny grains among the larger one, which shows an obvious non-uniformity. This microstructure may scatter phonons effectively but do not scatter carriers much [9,10].

Fig. 4 shows the electrical resistivity of the bulk samples measured from room temperature to 523 K. For all samples, with the increase of the temperature, the electrical resistivity increases, indicating a degenerated semiconductor behavior. The electrical resistivity of the Bi_2Te_3 is smallest. It is expected that rare earth elements doping can increase the electron concentrations and hence reduce the electrical resistivity. However, the electrical resistivity of $R_{0.2}Bi_{1.8}Te_3$ is higher than the un-doped Bi_2Te_3. The reason for this may be the reduction of the carrier mobility. Based on the equation $\rho = 1/\mu ne$, the electrical resistivity is inversely proportional to the carrier mobility μ and carrier concentration n, therefore the variations of n and μ will co-affect the variation of electrical resistivity. Lower carrier mobility will result in higher electrical resistivity, so the lower carrier mobility may be the reason for the increase of the electrical resistivity of the doped samples. There are two possible reasons for the lower carrier mobility of the doped samples. Firstly, rare earth element doping can decrease the carrier mobility due to intensifying alloying scattering. Secondly, the chemical bonds can influence the carrier mobility significantly. Generally, covalent bond is more favorable for the transport of carriers compared with ionic component [4]. Based on the traditional Pauling empirical formula and the electronegativities of both bonding atoms, the proportion of the ionic component of the A–B bond can be estimated by the equation of $1-\exp[-(x_A-x_B)^2/4]$, where x_A and x_B are electronegativities of A and B atoms, respectively [13]. According to the electro-negativities of cerium (1.12), yttrium (1.22), samarium (1.17), bismuth (2.02), and tellurium (2.10), it can be calculated that the RTe (21.3%, 17.6%, 19.4% for CeTe, YTe, SmTe, respectively) bond displays much more ionic component than the BiTe bond (0.16%), therefore $R_{0.2}Bi_{1.8}Te_3$ has more ionic component and will show a lower carrier mobility than Bi_2Te_3.

Fig. 5 shows the temperature dependences of Seebeck coefficients. All samples exhibit n-type conduction as they have the negative Seebeck coefficients in the measured temperature range, indicating that the Ce, Y, and Sm atoms substitution for the 6c positions of Bi in Bi_2Te_3 crystal cells should be a donor dopant. The intrinsic excitation of the $R_{0.2}Bi_{1.8}Te_3$ samples all occurs at about 480 K, implying that they have the similar band gaps and their intrinsic excitation temperatures are lower than that of binary Bi_2Te_3 (about 500 K). The Seebeck coefficients of all samples decrease with the increase of the temperature when temperature is beyond 480 K. This is due to the rapid increase of the minor carriers. The Seebeck coefficients of the $R_{0.2}Bi_{1.8}Te_3$ samples are all little lower than that of the Bi_2Te_3 sample. For metals or degenerate semiconductors (parabolic band, energy-independent scattering approximation [14]) the Seebeck coefficient is given by $\alpha = (8\pi^2 k_B^2/3eh^2)m^*T(\pi/3n)^{2/3}$ where k_B, h, m^*, and T are the Boltzmann constant, Planck constant, effect electron mass and absolute temperature, respectively [5]. Therefore, the variations of m^* and n will co-affect the variation of Seebeck coefficient. The m^* in the equation refers to the density-of-states effective mass, which increases with flat, narrow bands with high density of states at the Fermi surface. Rare-earth elements are intermetallic compounds. In these compounds, the 4f levels lie near the Fermi energy and form narrow non-parabolic bands, resulting in a large density of states at the Fermi level [5,15]. So for the $R_{0.2}Bi_{1.8}Te_3$ samples the m^* should be larger than that of the Bi_2Te_3. Based on the above equation, higher carrier concentrations will result in lower Seebeck coefficient. The lower Seebeck coefficients for $R_{0.2}Bi_{1.8}Te_3$ samples should be caused by higher carrier concentrations. The possible reason is as follows: the most common defects in Bi_2Te_3-based alloys include anti-site defects of Bi in Te-sites (Bi_{Te}, contributes one hole per defect), vacancies at the Te-sites (V_{Te}, contributes two electrons per defect) and vacancies at Bi-sites (V_{Bi}, contributes three holes per defect). Since the energy of evaporation for Te (52.55 kJ/mol) is much lower than that of Bi (104.80 kJ/mol), the evaporation of Te is much easier than that of Bi. The evaporation of each Te leaves one Te vacancy (V_{Te}) with two free electrons, as indicated in Equation $Bi_2Te_3 = 2Bi_{Bi}^{\times} + (3-x)Te_{Te}^{\times} + xTe(g) + xV_{Te}^{2+} + 2xe^-$ [16,17]. The dangling bonds at grain boundaries due to Te deficiencies can also be considered as fractional-V_{Te}, and also work as n-type doping in the same manner as the whole-V_{Te} defects inside the grains. So most fine-grained polycrystalline samples are therefore intrinsically n-type. Alloying with rare earth elements will decrease the concentration of anti-site defects at Te-sites [R_{Te} (R = Ce or Y and Sm)] which contributes one hole per defect and hence results in more electrons, due to the larger electronegative

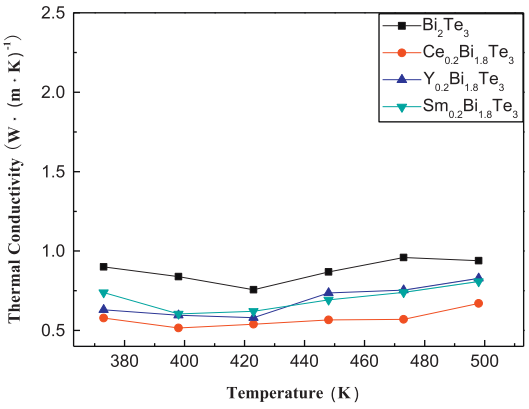

Fig. 6 Thermal conductivities of the hot-pressed samples.

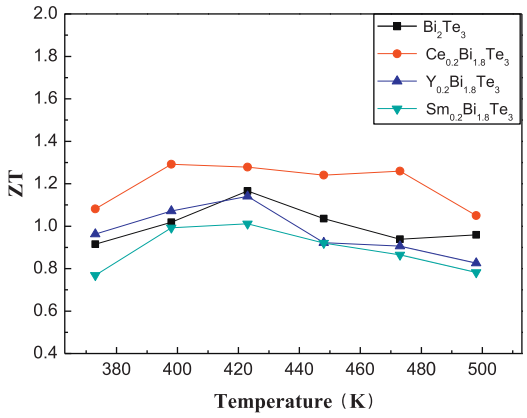

Fig. 7 *ZT* values of the hot-pressed samples.

difference between R (cerium (1.12), yttrium (1.22), samarium (1.17)) and Te (2.10) than between Bi (2.02) and Te (2.10).

Fig. 6 shows the thermal conductivities of the samples versus temperature. The thermal conductivities of the $R_{0.2}Bi_{1.8}Te_3$ samples are all lower than that of the Bi_2Te_3 in the measured temperature range. The reason may be that rare earth elements substituting for Bi in the $R_{0.2}Bi_{1.8}Te_3$ alloys introduced a number of point defects, which are expected to effectively reduce the short-wave phonon scattering and hence reduce the thermal conductivity. In addition, the grain sizes of the $R_{0.2}Bi_{1.8}Te_3$ bulks are all smaller than that of the Bi_2Te_3 bulks, as shown in Fig. 3, which should also be beneficial to decrease the thermal conductivity due to many interfaces exit.

The dimensionless figure of merit *ZT* was calculated by using the measured values of S, σ and κ as shown in Fig. 7. The *ZT* value of $Ce_{0.2}Bi_{1.8}Te_3$ is highest due to its lower thermal conductivity. All the values are higher than 1 in the measured temperature range and the peak value of 1.29 is achieved at 398 K, which is higher than zone melting ingots [16]. Such *ZT* characteristics are suitable for power generation applications because of a lack of available materials with high *ZT* in this temperature range. It indicates that Ce doping can indeed increase the figure merit of the Bi_2Te_3 thermoelectric alloy.

4. Conclusions

n-type $R_{0.2}Bi_{1.8}Te_3$ (R=Ce, Y and Sm) nanopowders were synthesized by the hydrothermal method and the thermoelectric properties of the bulk samples made by hot-pressing these nanopowders were investigated. Ce, Y and Sm doping has significant effects on the morphologies of the synthesized nanopowders. The possible reason may be that the replace of Bi by rare earth elements can change the bonds strength and affect the growth rate along *a*-axis, *b*-axis and *c*-axis. The Ce, Y and Sm doping will not be helpful to enhance the electrical resistivity and the Seebeck coefficients, but they will be helpful to reduce the thermal conductivity. Among these three elements the Ce doping seems to be more effective to reduce the thermal conductivity. As a result the *ZT* value of $Ce_{0.2}Bi_{1.8}Te_3$ can reach 1.29 at 398 K, which is not only much higher than other reported rare earth elements doping Bi_2Te_3-based alloy [18,19] but also higher than zone-melting ingots and other reported n-type Bi_2Te_3-based alloys [16,17,20]. The combined investigations of the element doping and nanostructure should be a focus for further developing novel thermoelectric materials.

References

[1] F.J. DiSalvo, Science 285 (1999) 703–706.
[2] T.M. Trit, Science 272 (1996) 1276–1277.
[3] L.E. Bell, Science 321 (2008) 1457–1461.
[4] G.J. Snyder, E.S. Toberer, Nature Materials 7 (2008) 105–114.
[5] Y.C. Lan, A.J. Minnich, G. Chen, Z.F. Ren, Advanced Functional Materials 20 (2010) 357–376.
[6] M.S. Dresselhaus, G. Chen, M.Y. Tang, R.G. Yang, H. Lee, D.Z. Wang, Z.F. Ren, J.P. Fleurial, P. Gogna, Advanced Materials 19 (2007) 1043–1053.
[7] G.Q. Zhang, Q.X. Yu, W. Wang, X.G. Li, Advanced Materials 22 (2010) 1–4.
[8] Z.G. Chen, G. Han, L. Yang, L. Cheng, J. Zou, Progress in Natural Science: Materials International 22 (2012) 535–549.
[9] W.J. Xie, J. He, H.J. Kang, X.F. Tang, S. Zhu, M. Laver, S.Y. Wang, J.R.D. Copley, C.M. Brown, Q.J. Zhang, T.M. Tritt, Nano Letters 10 (2010) 3283–3289.
[10] B. Poudel, Q. Hao, Y. Ma, Y. Lan, A. Minnich, B. Yu, X. Yan, D. Wang, A. Muto, D. Vashaee, X. Chen, J. Liu, M.S. Dresselhaus, G. Chen, Z. Ren, Science 320 (2008) 634–638.
[11] X.B. Zhao, X.H. Ji, Y.H. Zhang, T.J. Zhu, J.P. Tu, X.B. Zhang, Applied Physics Letters 86 (2005) 062111–062113.
[12] Y.C. Lan, A.J. Minnich, G. Chen, Z.F. Ren, Advanced Functional Materials 20 (2010) 357–376.
[13] M.L. Bhatia, Intermetallics 7 (1999) 641–651.
[14] M. Cutler, J.F. Leavy, R.L. Fitzpatrick, Physical Review 133 (1964) A1143–A1152.
[15] T.M. Tritt, M.A. Subramanian, MRS Bulletin 31 (2006) 188–194.
[16] S. Wang, W. Xie, H. Li, X. Tang, Intermetallics 19 (2011) 1024–1031.
[17] W.S. Liu, Q.Y. Zhang, Y.C. Lan, S. Chen, X. Yan, Q. Zhang, H. Wang, D.Z. Wang, G. Chen, Z.F. Ren, Advanced Energy Materials 1 (2011) 577–587.
[18] Y.H. Zhang, T.J. Zhu, J.P. Tu, X.B. Zhao, Materials Chemistry and Physics 103 (2007) 484–488.
[19] X.H. Ji, X.B. Zhao, H. Zhang, B.H. Lu, H.L. Ni, Journal of Alloys and Compounds 387 (2005) 282–286.
[20] X. Yan, B. Poudel, Y. Ma, W.S. Liu, G. Joshi, H. Wang, Y.C. Lan, D.Z. Wang, G. Chen, Z.F. Ren, Nano Letters 10 (2010) 3373–3378.